

1N-32 CR

4733B

7P

PROGRESS REPORT

High Spatial Resolution
Passive Microwave Sounding Systems

NASA Grant NAG 5-10

Covering the period
February 1, 1986 - July 30, 1986

Submitted by

David H. Staelin
Philip W. Rosenkranz
Pierino G. Bonanni
Albin W. Gasiewski

December 31, 1986

Massachusetts Institute of Technology
Research Laboratory of Electronics
Cambridge, Massachusetts 02139

(NASA-CR-180025) HIGH SPATIAL RESOLUTION
PASSIVE MICROWAVE SOUNDING SYSTEMS Progress
Report, 1 Feb. - 30 Jul. 1986 (Massachusetts
Inst. of Tech.) 7 p CSCL 20N

N87-14568

Unclas

G3/32 43758

High Spatial Resolution

Passive Microwave Sounding Systems

INTRODUCTION

The major activity during this period was conduct of two extensive series of flights aboard the ER-2 aircraft with the MIT 118-GHz imaging spectrometer together with a 53.6-GHz nadir channel and a TV camera record of the mission. Other microwave sensors, including a 183-GHz imaging spectrometer were flown simultaneously by other research groups.

Work also continued on evaluating the impact of high-resolution passive microwave soundings upon numerical weather prediction models, as described in the previous progress report. Evaluation of the results is under way and these will be described at length in the next report.

AIRCRAFT OBSERVATIONS

The instrument used for these observations is sketched in Fig. 1. The 118-GHz spectrometer was scanned by means of a rotating mirror driven by a stepper motor. The 7.5° beamwidth antenna pattern was swept across the track of the aircraft at 5.5-second intervals, imaging a swath 14 pixels wide. At an altitude of ~ 19.5 km this corresponds to a swath width of ~ 40 km at the terrestrial surface and somewhat less at altitudes typical of precipitation cells.

The stepper motor also can cause the radiometer to view two different black-body loads, one hot and one cold. The incoming radiation then passes through a chopper wheel and into the mixer-preamplifier portion of the system. The IF amplifier band of ~ 490 -2040 MHz is divided into seven passbands, each ~ 230 MHz wide. These passbands yield temperature weighting functions peaking at altitudes between ~ 170 mbar and the surface, as illustrated in Fig. 2. A

separate 53.6-GHz radiometer, also shown in Fig. 1, observes nadir with 7.5° beamwidth and a weighting function peaking near 500 mbar. The rms sensitivities of these radiometers are ~ 0.5 K for 0.22-sec integration, and less than 0.1 K with only modest spatial averaging; the system temperatures are roughly 1000 K. The spatial resolution of these images is typically ~ 2 -3 km at the surface and ~ 1.5 km at 8-km altitude. Figure 3 illustrates the detection of small (~ 6 km \times 6 km) precipitation cells which appear cold (white) over land; the dynamic range of these images is 8 K. Note that even these strong precipitation cells are not visible in the highest altitude temperature sounding channel (peaking near 170 mb).

In Fig. 4 are illustrated 118-GHz images obtained over ocean; the dynamic range is 2 K. At the top of the image a precipitation band appears warm (black) against the cooler background. The fact that this band is not seen in the three most opaque channels means that it is at altitudes lower than the tops of the convective cells in Fig. 3. Although it is difficult to see in this presentation format, Fig. 4 also displays what appear to be waves in the atmospheric temperature structure which are oriented roughly parallel with the front and which have a peak-to-peak amplitude of ~ 0.5 K. The wavelength is ~ 20 km. These waves become more apparent when the figure is viewed nearly tangentially and parallel to the wave fronts; they are most visible in the five most opaque channels. With improved filtering and presentation techniques such waves can be made more visible, and it should be possible to study their three-dimensional structure quantitatively.

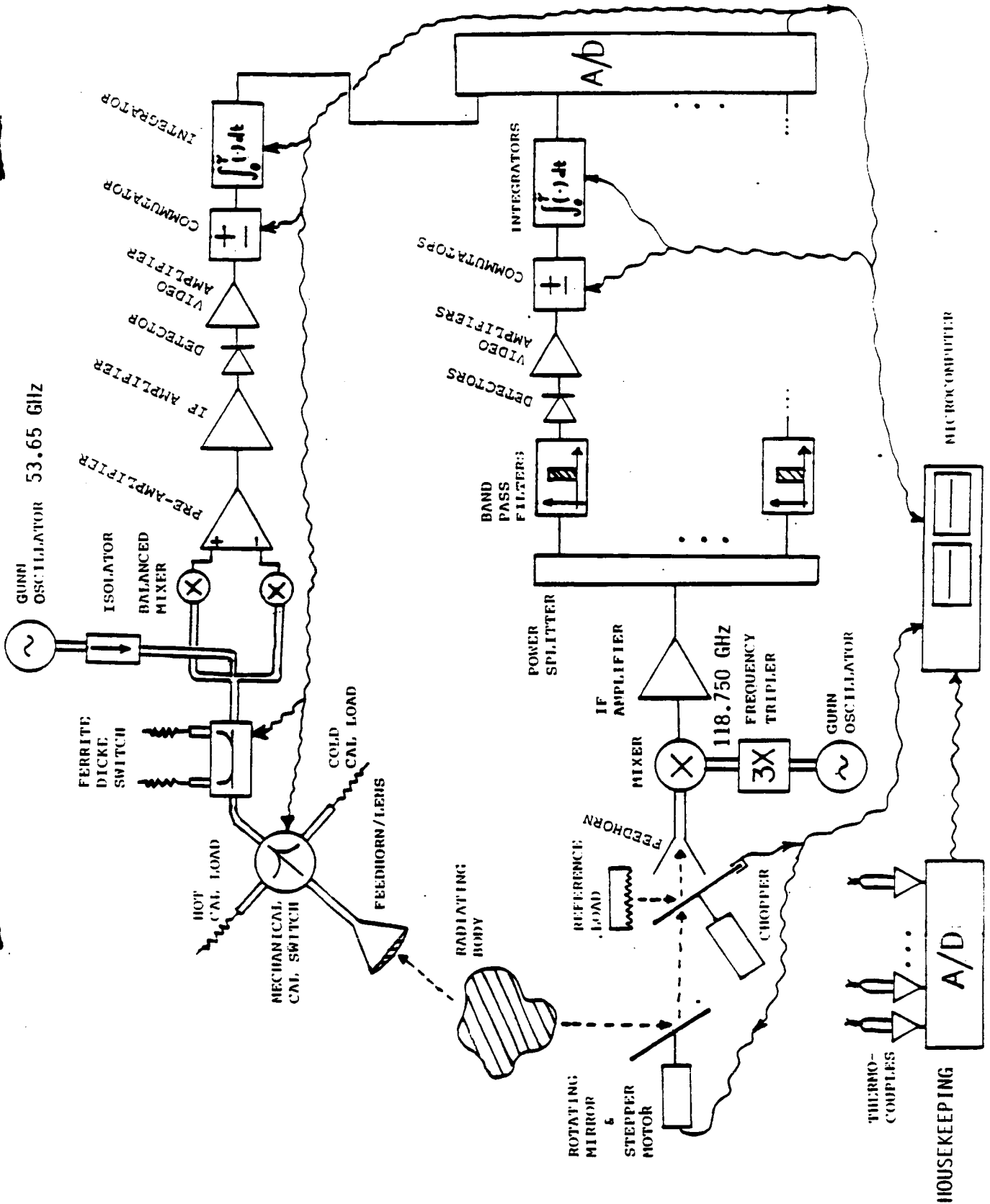


Figure 1. 118/53-GHz 7.5° beamwidth spectrometers. The 53.6-GHz channel views nadir and the 7-channel 118-GHz spectrometer scans laterally $\pm 45^\circ$ at 14 spots. The hot and cold 118-GHz calibration loads are viewed sequentially by the rotating mirror.

MTS DOWNWARD-LOOKING WEIGHTING FUNCTIONS

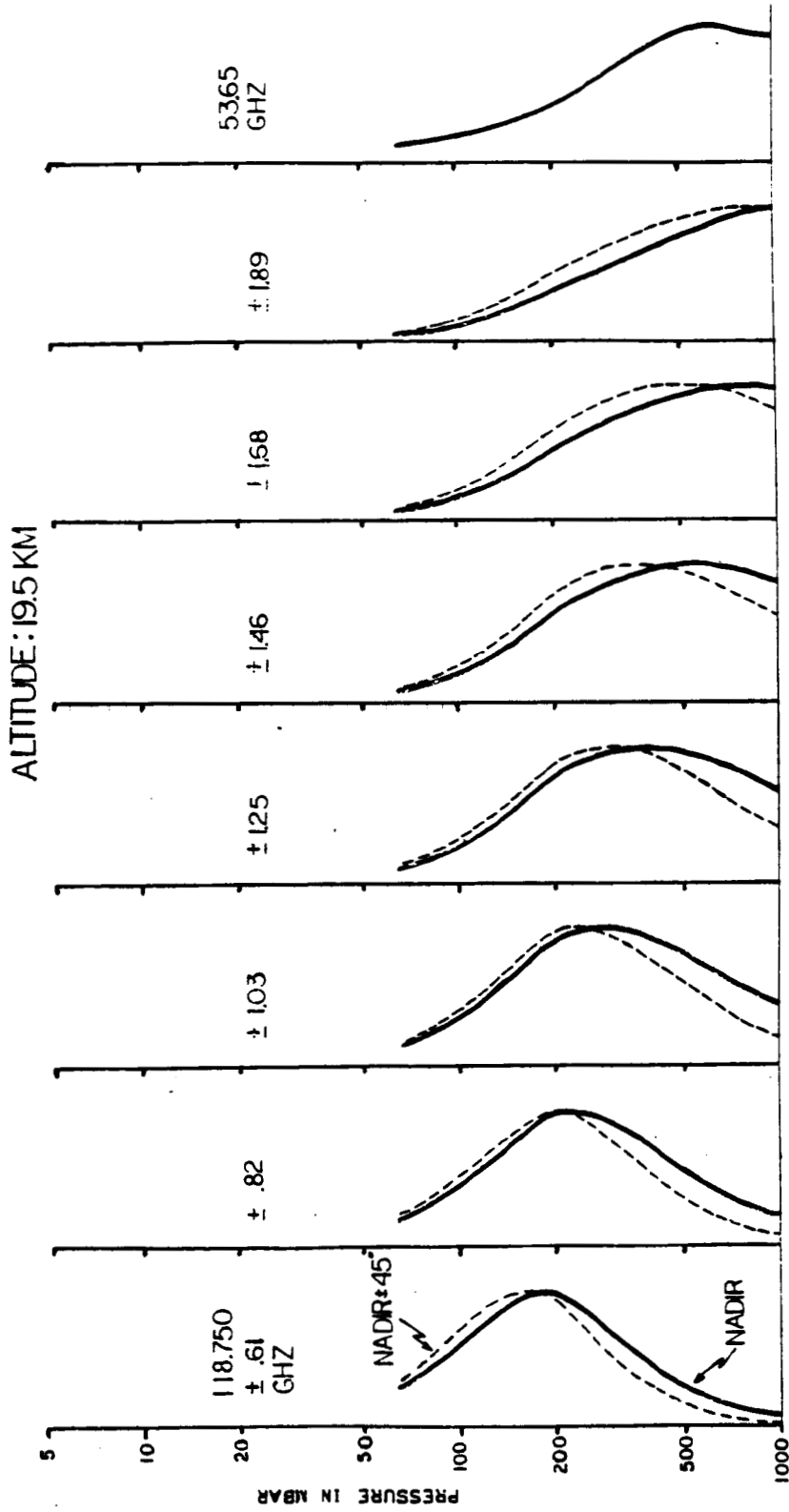


Figure 2. Temperature weighting functions for 7 channels near 118 GHz and one nadir-sounding channel centered at 53.65 GHz.

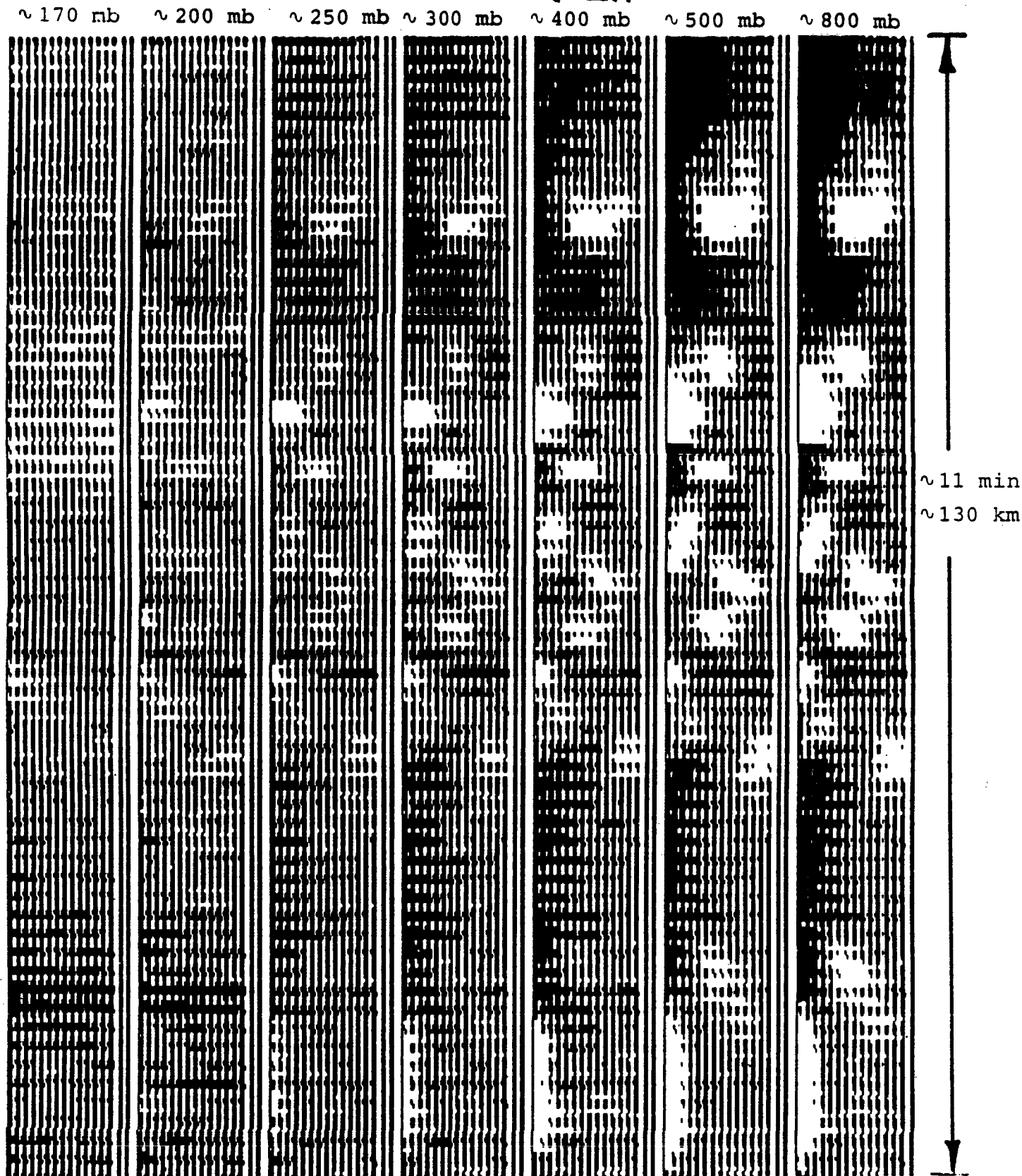


Figure 3. Preliminary 118-GHz images of convective precipitation cells (white) over land. The dynamic range is 8 K and the white spots are cold. Each swath is ~ 40 km wide at the terrestrial surface and ~ 22 km at 8-km altitude; therefore typical cell diameters here are ~ 6 km. The swaths correspond to temperature weighting functions peaking near 170, 200, 250, 300, 400, 500, and 800 mbar, left to right, respectively.

ORIGINAL PAGE IS
OF POOR QUALITY

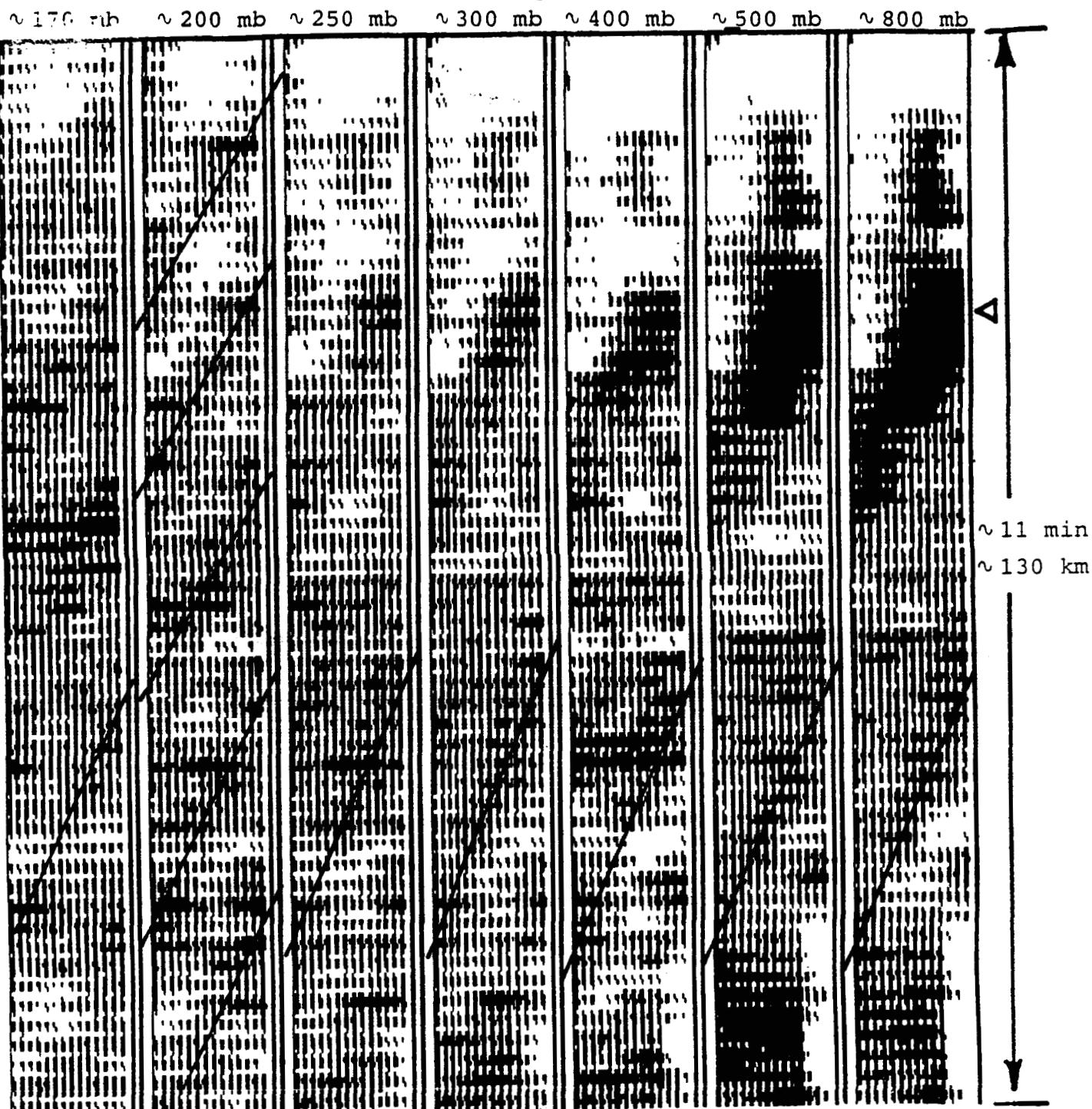


Figure 4. Preliminary 118-GHz images of a front over ocean exhibiting a rain band (black, marked by a triangle) and apparent temperature waves with $\lambda \approx 20$ km (selected wavefronts are marked by straight lines). The dynamic range is 2 K and black is warm. The approximate altitude where each temperature weighting function peaks is indicated at the top of each image. The swath width at the surface is ~ 40 km, and at 8-km altitude it is ~ 22 km.